Femtosecond laser induced damage characterization of transmission volume phase gratings

Ó. Martínez-Matos,[1,a)] M. P. Hernández-Garay,[1] J. G. Izquierdo,[2] P. Vaveliuk,[3,4] L. Bañares,[2] and M. L. Calvo[1]

[1]*Facultad de Ciencias Físicas, Universidad Complutense de Madrid, Ciudad Universitaria s/n, Madrid 28040, Spain*
[2]*Departamento de Química Física I and Centro de Láseres Ultrarrápidos, Facultad de Ciencias Químicas, Universidad Complutense de Madrid, Ciudad Universitaria s/n, Madrid 28040, Spain*
[3]*Facultade de Tecnologia, Servicio Nacional de Aprendizagen Industrial SENAI-Cimatec, Av. Orlando Gomes 1845, 41650-010 Salvador, Bahia, Brazil*
[4]*Centro de Investigaciones Ópticas (CONICET La Plata-CIC), Cno. Centenario y 506, P.O. Box 3, 1897 Gonnet, Argentina*

(Received 8 July 2014; accepted 22 July 2014; published online 30 July 2014)

A procedure to characterize the induced damage and the incubation effects in volume transmission gratings under femtosecond laser pulse train illumination is presented. It was also developed a formalism that explains the damage processes. Our proposal was employed on glass gratings to show the effectiveness of the method and its potential to design transmission gratings with enhanced laser induced damage threshold. This procedure is able to be extended to any transmission grating composed by chemically non-uniform material, opening up new perspectives to femtosecond laser pulse shaping. © *2014 AIP Publishing LLC*.
[http://dx.doi.org/10.1063/1.4892010]

Diffraction gratings are essential parts of femtosecond laser systems. They are used as dispersive elements in compressors and stretchers as well as for temporal, spatial, and spectral pulse shaping, to name a few. A laser induced-damage threshold (LIDT) characterization of gratings, i.e., the highest fluence value for which no damage is produced, is a main task to determine its applicability range. In the last years, LIDT in reflection multilayer dielectric gratings[1–3] and in mixed metal dielectric gratings[4] has been investigated by varying the material composition of the multilayer and by proving different grating profiles. The damage dynamics were established for a wide class of gratings, but only in the reflection geometry. No research on LIDT has been reported in the transmission geometry at the present time. In this Letter, we propose a procedure to characterize the induced damage and the incubation effects, i.e., permanent material changes produced by multiple pulse accumulation mechanisms, in volume transmission gratings when implemented in a femtosecond laser system. Besides, we develop a formalism to explain the damage processes. Our approach is tested on a photopolymerizable glass grating, showing the validity of the method to design transmission gratings with enhanced LIDT.

The analysis is based on the photopolymerizable glass[5–9] because the transmission gratings on this type of material have been implemented to spatial[10] and spectral[11] pulse shaping in a femtosecond laser system. We start with the grating characterization. The grating is formed by a permanent spatial modulation of the refractive index, $n(x) = n_b + n_1(x)$, within the bulk of the glass. Parameter n_b is the background refractive index of the insulating binder (the glass) and

$$n_1(x) = n_0 + \Delta n_0 \cos\left(\frac{2\pi}{\Lambda}x\right) \tag{1}$$

is the refractive index due to a periodic distribution of polymer and Zr-species concentration in this material.[5] These species, called the modulating species (MS), modulate the refractive index. Locations of maximum (minimum) concentration of MS reach the maximum (minimum) values of the refractive index. The parameters n_0 and Δn_0 are the background and the modulation of the refractive index due to the periodic distribution of MS, while Λ is the grating period and x is the modulation axis. We distinguish between the background refractive indexes n_b and n_0 because they are related to different chemical components, the former much more resistant to damage that the latter. Thus, it is expected that damage appears on locations of maximum MS concentration when the grating is illuminated with plane-wave pulses. The gratings studied in this work have the following characteristics: thickness $\sim 100\,\mu$m, $\Lambda = 2\,\mu$m, $n_b \sim 1.55$, $n_0 \sim 2 \times 10^{-3}$, and $\Delta n \sim 2 \times 10^{-3}$.

LIDT was studied by irradiating the gratings with a train of pulses from an amplified Ti:sapphire femtosecond laser centered at $\lambda_c = 800\,$nm, at 1 kHz repetition rate, and with 50 fs pulse duration. In these studies, pulse fluence was below the single pulse damage threshold to investigate incubation effects. The procedure for damage characterization proposed in this Letter consists in two complementary experimental setups (see Fig. 1). In a first experiment (exp. 1), the incidence of the pulsed laser was normal to the grating plane to avoid diffraction. Damage processes were derived from the results of this experiment. In a second experiment (exp. 2), the incoming laser beam impinged the grating at Bragg

[a)]Author to whom correspondence should be addressed. Electronic mail: omartine@fis.ucm.es

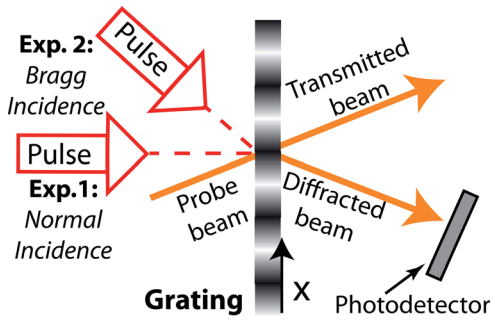

FIG. 1. The two different experimental setups to measure the incubation effect and the LIDT.

condition for λ_c, generating a diffracted pulse that interferes with the incident pulse in the bulk of the grating. This is the configuration used to investigate the interference effects on damage threshold. In both experiments, the gratings were altered by an incubation effect that varies the refractive index modulation. These changes were monitored by measuring the diffraction efficiency, η, of a continuous wave He-Ne probe beam under Bragg incidence (BI) (see Fig. 1). The η is related to the total refractive index modulation, $\Delta n_0 + \Delta n(N)$, through the coupled wave theory,[12] where $\Delta n(N)$ is the induced refractive index modulation by pulses irradiation. Hence, the evolution of the grating strength is obtained from these measurements as a function of the number of pulses, N.

Let us first discuss the results obtained from exp. 1. Fig. 2(a) displays $\Delta n(N)$ for laser fluences 0.061, 0.090, and 0.123 J/cm^2. In all the cases, $\Delta n(N)$ goes through two regimes. In the first regime, $\Delta n(N)$ increases linearly with increasing N due to the incubation effects up to a critical pulse number, N_D. At this point, the curves depart from the linear behavior due to the formation of defects that scatters light. Damage takes place from N_D, comprising the second regime.

At the linear regime, the grating exhibits a permanent change due to the incubation effect while the optical quality of the material is preserved. No induced scattering is detected. The $\Delta n(N)$-slope is represented in Fig. 2(b) as a function of laser fluence, ϕ. The quadratic function $\partial \Delta n(N)/\partial N = \Delta n_0\, \beta\, \phi^2$ fits properly the experimental data (line in Fig. 2(b)), with $\beta = (5.5 \pm 0.5) 10^{-2} \frac{\text{cm}^4}{J^2 N}$. The constant Δn_0 is introduced in the fitting for convenience. Hence, the induced refractive index modulation behaves as $\Delta n(N) = \Delta n_0\, \beta\, \phi^2 N$, showing that is linear with respect to the pulse number and quadratic with respect to the fluence. Thereby, $\Delta n(N)$ can be increased in a controllable fashion just by impinging the grating with the proper number of pulses. By this procedure, it is possible to modify Δn without altering the optical quality of the material.

The quadratic dependence of $\Delta n(N)$, with the fluence ϕ, suggests that the incubation effect is dominated by a two photon absorption process. Electronic transitions to the conduction band from nearby energy levels are responsible of the variation of the refractive index. These levels, localized between the valence and the conduction bands of the binder, can be associated to the presence of MS, which are distributed periodically in the bulk according to $n_1(x)$. The maximum MS concentration is reached at locations $x_{NI} = m\Lambda$ (where m is an integer and the sub-index NI refers to normal incidence), where $n_1(x_{NI})$ is the maximum index value. At these places, there are more density of intraband energy levels increasing the probability of a photoinduced electronic transition to the conduction band. Once the transition occurs, the MS is chemically altered or/and a local stress is induced. Taking into account these assumptions, the refractive index evolves with the number of pulses at normal incidence as

$$n_1(x,N) = n_1(x) + n_{NI}(x,N), \tag{2}$$

where

$$n_{NI}(x,N) = n_1(x)\beta\, \phi^2 N \tag{3}$$

is the induced refractive index due to the incubation effect. This incubation mechanism explains the change in Δn at the

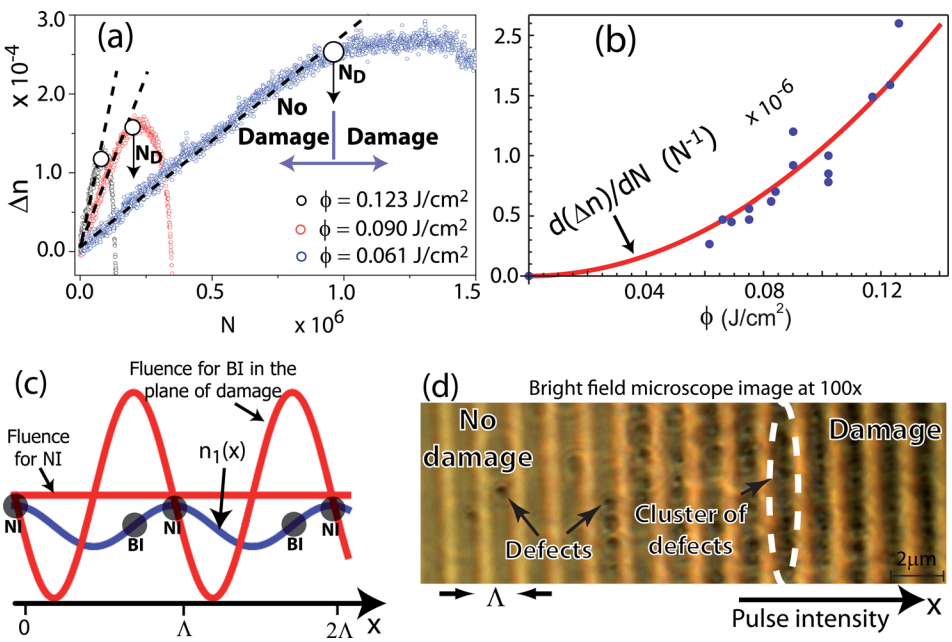

FIG. 2. (a) $\Delta n(N)$ as a function of the pulse number, N, at normal incidence for different pulse fluences. Dotted lines represent the linear stage and N_D the critical pulse number from which the sample is damaged. (b) Points representing the $\Delta n(N)$-slope in terms of ϕ that are well fitted by a quadratic function. (c) Pulse effective fluence in the bulk of the grating for normal incidence (NI) and for Bragg incidence (BI) in the *plane of damage*. Black circles represent defect formation under NI and BI. (d) Microscope image of the grating after damage when illuminated with non-uniform intensity pulses. The arrow points the direction of increasing intensity.

linear regime, in a similar fashion to the recently proposed for poly(methyl methacrylate).[13]

In the non-linear regime, bulk damage for normal incidence was detected by the generation of induced defects, created from the critical pulse number N_D. They appear periodically at the same positions x_{NI} of maximum change due to the incubation effect. Fig. 2(c) schematically shows that the defects are on positions x_{NI}, on the crests of function $n_1(x)$. In Fig. 2(d), a microscope image of the photopolymerizable glass grating after damage is shown. The black points, identified as the defects, appear at positions x_{NI}. Defect density increases with the pulse fluence by the formation of defect clusters on x_{NI}. Thus, the damage process can be interpreted as follows: the modified material by the incubation effect leads to seed electrons for free electron density by photo-ionization and avalanche ionization. The maximum number of seed electrons is reached at x_{NI}, expecting damage to appear at these locations. At the pulse number N_D, the electrons in the conduction band reach a critical density[14] and damage takes place at positions x_{NI} due to a runaway absorption mechanism that generates defects. As a consequence, the gratings are less resistant to irradiation on x_{NI} than in other locations $x \neq x_{NI}$.

Damage generated by the incubation effect has been properly interpreted for chemically uniform materials by means of a probabilistic model. It has been applied to ns-[15] and fs-pulse irradiation for various uniform material classes.[16–19] Based on this model, we develop a formalism to interpret the damage mechanism to chemically non-uniform materials, including the case of transmission gratings. For the photopolymerizable glass grating, its chemical composition changes locally with the variation of the MS concentration. The probabilistic model relates the single-pulse damage threshold, ϕ_1, with the multiple pulse damage threshold, ϕ_N, via

$$\phi_N = \phi_1 N_D^{\xi-1}, \tag{4}$$

where the parameter ξ is a material-dependent coefficient called *degree of incubation*. The value ξ is associated to an accumulation of energy in the material by mechanical or chemical mechanisms while the sample is irradiated. A value of $\xi = 1$ suggests the absence of incubation, although for $\xi < 1$ incubation effects are present. For $\xi > 1$, the material becomes more resistant to damage as the pulses etch it.

The damage threshold fluence, ϕ_N, as a function of the critical pulse number N_D is represented by green circles in Fig. 3. The line is the fitting using the probabilistic model with coefficients $\phi_1 = (0.76 \pm 0.08)\,\mathrm{J/cm^2}$ and $\xi = 0.827 \pm 0.008$, supporting the applicability of this model to our results. An incubation effect takes place in the photopolymerizable glass that lower the damage threshold fluence for subsequent pulses ($\xi < 1$). The fitting values (ϕ_1, ξ) are close to those found in uniform materials, see, for example, Refs. 16–19. Notice that since damage occurs at x_{NI}, the LIDT found in the photopolymerizable glass refers to damage threshold on the less resistant locations to irradiation. We underline that places where $x \neq x_{NI}$ are no damaged. This is the main difference with respect to chemically uniform materials in which damage occurs uniformly in the sample.

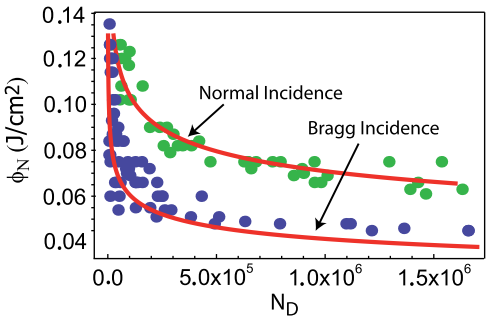

FIG. 3. LIDT for NI (green circles) and BI (blue circles) incidence and the fitting to the probabilistic model (solid lines) using Eqs. (4) and (9), respectively. Interference effects reduce the LIDT for Bragg incidence.

The highest possible value of the induced refractive index on locations where damage starts, n_{dmg}, is calculated evaluating Eq. (3) at x_{NI} for the critical pulse number N_D. Taking into account Eq. (4), we find

$$n_{dmg}\,\phi_N^{\frac{2\xi-1}{1-\xi}} = C, \tag{5}$$

where $C = (n_0 + \Delta n_0)\beta\phi_1^{\frac{1}{1-\xi}}$ is a constant whose value is established by the type of material. This expression balances the increased refractive index, just before damage, with the multiple pulse damage threshold, ϕ_N. If Eq. (5) is satisfied, damage takes place. We underlay that n_{dmg} is related to the density of seed electrons for damage to take place when the grating is irradiated with pulses with fluence ϕ_N. Whenever the critical density is reached for a giving ϕ_N, damage takes place, irrespectively on the physical mechanism reaching the critical density of seed electrons and on its specific location in the grating. For this reason, Eq. (5) is always satisfied independent on the geometry of excitation, being the distinctive trait of the grating. In the following, we will apply this assumption to find the damage threshold and the locations of damage when the transmission gratings are irradiated under Bragg incidence, exp. 2.

In exp. 2, a femtosecond pulse train of fluence ϕ impinges the grating at Bragg incidence (BI) generating a diffracted pulse whose intensity increases as it propagates in the bulk. In particular, there is a plane (parallel to the grating surface), namely, the *plane of damage*, in which the incident and diffracted pulses reach the same fluence, $\phi/2$. It occurs if the diffraction efficiency of the grating is higher than 50%, what is meeting in all experiments. The interference profile generated by pulses with fluence $\phi/2$ can be expressed by means of an effective fluence, ϕ_{eff}, as

$$\phi_{eff}(x) = \phi\left[1 - \sin\left(\frac{2\pi}{\Lambda}x\right)\right]. \tag{6}$$

Therefore, the highest effective fluence in the bulk, 2ϕ, is reached at the *plane of damage* at positions $x = \Lambda(m - 1/4)$. It is expected that damage starts at this plane. Notice that $\phi_{eff}(x)$ and $n_1(x)$ are shifted due to a $3\pi/2$ dephasing between the incident and diffracted pulses. The origin of the dephasing comes from the imaginary constant $-i$ on the amplitude of the diffracted beam calculated using the well-known coupled wave theory.[12] This shift generates damage

on locations different than those corresponding to normal incidence.

Following the procedure to obtain Eq. (3), the induced refractive index for BI, $n_{BI}(x,N)$, at the *plane of damage*, evolves with N as

$$n_{BI}(x,N) = n_1(x)\,\beta\phi_{eff}^2(x)\,N. \tag{7}$$

Notice that in most cases $n_{BI}(x,N) \neq n_{NI}(x,N)$. Then, considering the induced refractive index and the effective fluence at the plane of damage, Eq. (5) applied to BI takes the form:

$$n_{BI}(x_{BI},N_D)\phi_{eff}^{\frac{2\xi-1}{1-\xi}}(x_{BI}) = C. \tag{8}$$

The x_{BI} are the locations where damage starts. These positions are found maximizing the left side of Eq. (8) on the variable x. This ensures that Eq. (8) is satisfied with the less number of pulses, thereby, the locations x_{BI} are firstly damaged. Specifically, we find $x_{BI} \sim \Lambda(m-1/4)$. These locations correspond to the peak intensity due to interference effects and they are schematically represented by the BI points in Fig. 2(c). Damage appears shifted by $-\pi/4$ radians with respect to the normal incidence. For instance, damage at peak intensities due to interference effects has also been demonstrated in reflection gratings.[1–4] This damage mechanism is the main limitation on damage threshold for transmission gratings and for reflection gratings as well. Furthermore, the probabilistic model for Bragg incidence is determined substituting Eqs. (6) and (7) in Eq. (8), evaluated on locations x_{BI}

$$\phi_N = \phi_{1,eff}\,N_D^{\xi-1}, \tag{9}$$

where $\phi_{1,eff} = \phi_1/2 \times [n_0/(n_0+\Delta n_0)]^{\xi-1}$. The grating behaves as at normal incidence but with an effective single-pulse damage threshold given by $\phi_{1,eff}$. This value differs from that considering only the effective fluence in the bulk, $\phi_1/2$. In fact, the ratio $n_0/(n_0+\Delta n_0) \equiv n_1(x_{BI})/n_1(x_{NI})$ states that damage for both, Bragg and normal incidences, starts at locations where the chemical composition of the gratings (MS concentration) are different. A way to increase the LIDT for Bragg incidence must maximize $\phi_{1,eff}$. This could be achieved recording gratings with high refractive index modulation, Δn_0, for materials with $\xi < 1$. This simple solution is a great advantage when comparing to multilayer gratings in which LIDT enhancement is reached with the decrease of the electric field inside the dielectric pillar.[3] In this process, the grating performance is diminished. Blue circles in Fig. 3 display the experimental data for damage threshold at Bragg incidence. The LIDT is considerably reduced due to pulse interference, in accordance with the proposed model. The red line in the figure is the representation of (9) with the parameters found for normal incidence. Notice that the fitting is in good agreement with experimental data, enhancing that there is no adjustable parameters. This is a strong indication on both, the effectiveness of the proposed procedure and the validity of our formalism applied to volume transmission gratings.

In summary, we have presented a method to characterize both the incubation effect and the damage mechanisms on transmission volume phase gratings when irradiated with a train of femtosecond pulses. The procedure consists on two complementary irradiation setups. Irradiation under normal incidence reveals the damage processes, while irradiation under Bragg condition is used to analyze the interference effects on damage threshold. The experimental results have been interpreted by means of a formalism that is an extension of the probabilistic model to chemically non-uniform materials. This provides a efficient method to design transmission gratings with enhanced LIDT. Application to the photopolymerizable glass reveals a greater resistance to damage when the refractive index modulation is increased. This methodology can be implemented to other materials, making volume gratings working in transmission geometry attractive to high intensity femtosecond laser applications.

We thank J. A. Rodrigo and T. Alieva for valuable discussions and advice. We thank the financial support from the Spanish Ministerio de Economía y Competividad under Projects TEC 2011-23629, CTQ2008-02578/BQU, and CTQ2012-37404-C02-01 and Consolider program SAUUL CSD2007-00013 and from *Conselho Nacional de Desenvolvimento*. The facilities provided by the Center of Ultrashort Lasers at Madrid Complutense University are gratefully acknowledged.

[1]J. Neauport, E. Lavastre, G. Razé, G. Dupuy, N. Bonod, M. Balas, G. de Villele, J. Flamand, S. Kaladgew, and F. Desserouer, Opt. Express **15**, 12508 (2007).
[2]L. Gallais, B. Mangote, M. Zerrad, M. Commandré, A. Melninkaitis, J. Mirauskas, M. Jeskevic, and V. Sirutkaitis, Appl. Opt. **50**, C178 (2011).
[3]S. Hocquet, J. Neauport, and N. Bonod, Appl. Phys. Lett. **99**, 061101 (2011).
[4]J. Neauport, N. Bonod, S. Hocquet, S. Palmier, and G. Dupuy, Opt. Express **18**, 23776 (2010).
[5]F. del Monte, O. Martínez-Matos, J. A. Rodrigo, M. L. Calvo, and P. Cheben, Adv. Mater. **18**, 2014 (2006).
[6]O. Martinez-Matos, M. L. Calvo, J. A. Rodrigo, P. Cheben, and F. del Monte, Appl. Phys. Lett. **91**, 141115 (2007).
[7]M. L. Calvo and P. Cheben, J. Opt. A: Pure Appl. Opt. **11**, 024009 (2009).
[8]O. Martinez-Matos, J. A. Rodrigo, M. L. Calvo, and P. Cheben, Opt. Lett. **34**, 485 (2009).
[9]A. V. Velasco, M. L. Calvo, and P. Cheben, J. Appl. Phys. **113**, 033101 (2013).
[10]O. Martínez-Matos, J. A. Rodrigo, M. P. Hernández-Garay, J. G. Izquierdo, R. Weigand, M. L. Calvo, P. Cheben, P. Vaveliuk, and L. Bañares, Opt. Lett. **35**, 652 (2010).
[11]M. P. Hernández-Garay, O. Martínez-Matos, J. G. Izquierdo, M. L. Calvo, P. Vaveliuk, P. Cheben, and L. Bañares, Opt. Express **19**, 1516 (2011).
[12]H. Kogelnik, Bell Syst. Tech. J. **48**, 2909 (1969).
[13]A. Baum, P. J. Scully, W. Perrie, D. Jones, R. Issac, and D. A. Jaroszynski, Opt. Lett. **33**, 651 (2008).
[14]N. Bloenbergen, IEEE J. Quantum Electron. **10**, 375 (1974).
[15]Y. Jee, M. F. Becker, and R. M. Walser, J. Opt. Soc. Am. B **5**, 648 (1988).
[16]S. Gaspard, M. Forster, C. Huber, C. Zafiu, G. Trettenhahn, W. Kautek, and M. Castillejo, Phys. Chem. Chem. Phys. **10**, 6174 (2008).
[17]J. Bonse, S. M. Wiggins, J. Solis, H. Sturm, L. Urech, A. Wokaun, and T. Lippert, J. Phys.: Conf. Ser. **59**, 105–111 (2007).
[18]L. M. Machado, R. E. Samad, W. de Rossi, and N. D. V. Junior, Opt. Express **20**, 4114 (2012).
[19]S. Baudach, J. Bonse, and W. Kautek, Appl. Phys. A **69**, S395 (1999).